REACTOR RELEVANT ICRF HEATING IN JET D-T PLASMAS

The JET Team[1]
(presented by D.F.H. Start [2])

JET Joint Undertaking,
Abingdon, Oxfordshire,
United Kingdom.

Abstract

Ion Cyclotron Resonance Heating (ICRH) experiments have been carried out in reactor relevant scenarios during the Deuterium-Tritium (DTE1) campaign in JET. For the first time it has been possible to assess the deuterium minority in tritium plasmas (D)T scheme: this produced a steady-state DT fusion power up to 1.66 MW for input ICRF power of 6 MW. Strong ion heating, with core ion temperature up to 13 keV, has been observed when using ^{3}He minority heating in both 50:50 D-T and tritium dominated H-mode plasmas. Second harmonic tritium heating has also been studied and, as expected for JET plasma conditions, it has produced mainly electron heating. Finally, the inverted scenario of tritium minority in deuterium (T)D was successfully demonstrated.

1. INTRODUCTION

Ion cyclotron resonance heating (ICRH) is the only method of additionally heating ions in the dense core of a tokamak reactor. Radio Frequency (RF) power is used to excite a fast magnetosonic wave, to which the high density plasma is accessible. The wave is absorbed at a cyclotron resonance which is positioned in major radius (usually the plasma centre) by the choice of magnetic field and RF frequency. The ions damping the wave are often accelerated to suprathermal energies. This energy is then transferred to the thermal ions and electrons by Coulomb collisions. If the energy of the absorbing ions is less than a critical value, E_{CRIT} , power flows more to the thermal ions than to the electrons.

The ICRH system on JET has been designed to operate with a wide range of fundamental and multiple harmonic scenarios, with the frequency band covering the range 23 MHz to 56 MHz [1]. The versatility of the system was exploited in the recent JET experiments with D-T plasmas which provided a unique opportunity to assess the physics and performance of ICRH schemes that are relevant to a fusion reactor. These schemes comprise ^{3}He and deuterium minority ions at their fundamental resonances and tritium majority ions at their second harmonic resonance. In addition, tritium minority heating experiments were carried out with 5% tritium in 95% deuterium plasmas. The experiments were carried out in H-mode plasmas, except for the tritium minority studies where the available power was below the H-mode threshold, in single-null X-point configurations.

2. FUNDAMENTAL DEUTERIUM MINORITY HEATING.

The potential of the deuterium minority in tritium, (D)T, ICRF scenario for both plasma heating and for generating fusion power through suprathermal reactions has previously been recognised [2, 3]. Theoretical calculations for reactor conditions [4] suggest that, with $k_{//} \approx 4\ m^{-1}$, deuterium concentrations $\eta_D = n_D / (n_D+n_T)$ around 30% will provide bulk ion heating. For higher η_D , direct electron damping will become a competitor to the deuterium cyclotron absorption. For JET conditions, theory predicted that η_D between 10% and 20% would produce maximum reactivity [3,5]. The D(T) scheme was tested and optimised for the first time in the JET D-T campaign. The experiments were carried out at a frequency of 28 MHz and a toroidal magnetic field of 3.7 T to give central RF power deposition, with plasma currents I_p = 3.3 MA and 3.7 MA and RF power up to 6 MW.

---

1 see Appendix to IAEA-CN-69/OV1/2, The JET Team (presented by M.L. Watkins)

2 This paper summarises the extensive programme of ICRH experiments in D-T plasmas initiated and carried out by Dr. David Start, who died suddenly in August 1998. The paper has been completed by G.A. Cottrell and F.G. Rimini.

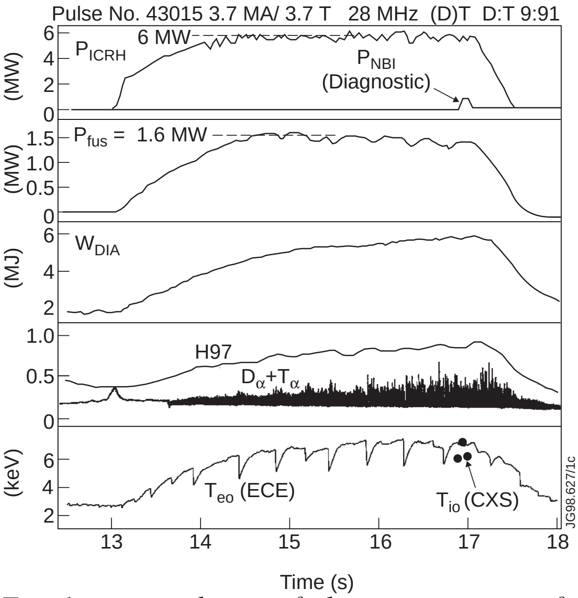

Fig. 1. time evolution of plasma parameters for record fusion (D)T scenario.

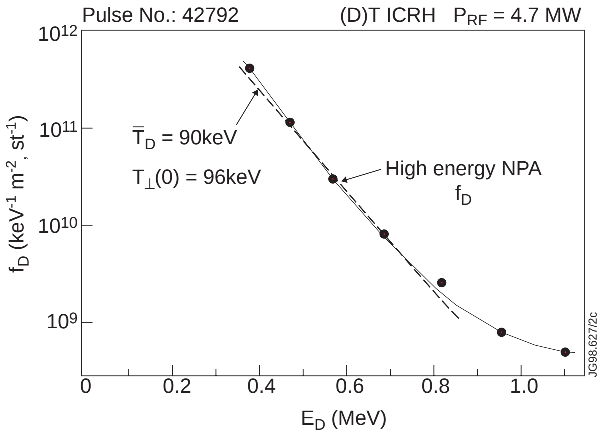

Fig. 2. NPA line integral deuteron distribution function for discharge 42792 (I_p=3.7 MA, B_T=3.7 T).

The fusion reactivity between the suprathermal deuterons and the thermal tritons was maximised by achieving an average deuteron energy close to 120 keV, close to the peak of the D-T fusion rate. The highest reactivity is achieved in H-mode plasmas with ICRF power of 6 MW, a D:T ratio of 9:91 and a core electron density $\sim 5 \times 10^{19}$ m^{-3} (Fig.1). The fusion power reaches 1.66 MW and the fusion figure of merit, $Q_{IN} = P_{fus}/(P_{RF} + P_{OH})$, was 0.22 over a period of 2.7s, corresponding to three energy replacement times. The length of the RF pulse was limited due to neutron economy. Here P_{fus}, P_{RF} and P_{OH} are the output fusion power, the input RF and ohmic heating powers, respectively. The time duration of the ICRF pulse was mainly dictated by neutron economy. The frequency of the small amplitude ELMs is about 250 Hz, and the ratio of the ELM repetition time and the confinement time (0.87s) gives an upper limit of 0.5% to the fraction of the plasma energy content ($\Delta W/W$) transferred by each ELM across the scrape-off layer. The energy confinement time, τ_E = 0.87s, corresponds to an ELMy H-mode quality factor, ITERH97-P [6], of 0.90.

The electron and ion temperatures are measured by Electron Cyclotron Eemission (ECE) and Charge Exchange Spectroscopy (CXS), which uses tritium neutral beam power up to 2.3 MW to give sufficient signal from the plasma centre. The central ion temperature, $T_i(0)$, is close to the central electron temperature, $T_e(0)$, showing the presence of substantial bulk ion heating by the deuterons. Such ion heating is expected since the deuteron energy (E_{crit}) which gives equal collisional power transfer to the ions and electrons is 100 keV for an electron temperature of 7 keV. The predicted fusion reactivity using the PION code [7] is in excellent agreement with the observed reactivity. The power partition calculations predict that 70% of the power is absorbed by the deuterons, 15% by carbon plus beryllium impurities, 10% by direct electron damping and 5% by mode conversion. The direct electron absorption occurs through a combination of Transit Time Magnetic Pumping (TTMP) and Electron Landau Damping (ELD). Summing the components, including the ohmic heating, gives a ratio of ion to electron heating of 45:55.

An estimate of the deuteron energy can be obtained from the Doppler broadening of the 14 MeV neutron energy spectrum and from Neutral Particle Analysis (NPA) in the energy range 0.3 - 1.1 MeV [8]. The neutron data for discharge 43015 show a deuteron energy of 125 ± 25 keV, while the deuteron velocity distribution given by NPA for discharge 42792, which produced 1.2 MW of fusion power with an RF power of 4.7 MW, is shown in Fig. 2. The tail temperature is about 96 keV, in good agreement with the neutron spectroscopy measurement of 100 keV for this discharge (Fig.4).

To maximise the fusion reactivity, η_D was varied between 9% and 22%. The fusion yield was highest at 9% but the highest values of $T_i(0)$ and the strongest ion heating occurred at larger concentrations, where there is substantial evidence for a transfer of power absorption away from the suprathermal

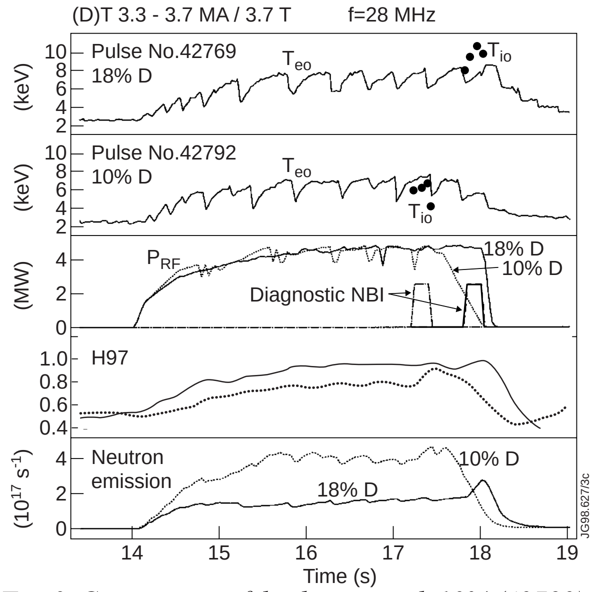

Fig. 3. Comparison of discharges with 10% (42792) 18 % deuterium fraction (42769).

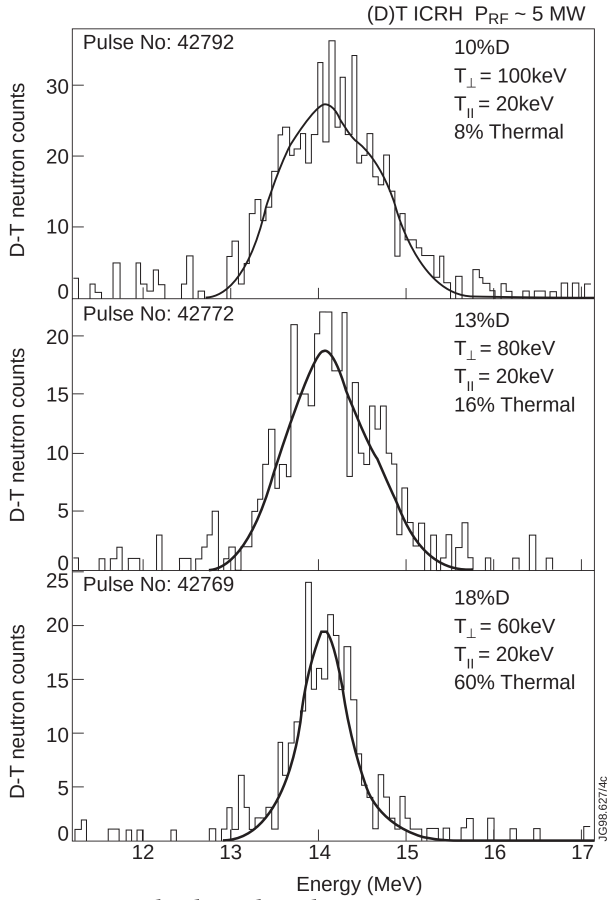

Fig. 4. Doppler broadened neutron energy spectra for (D)T ICRH.

deuterons towards a strong central bulk ion heating mechanism. The first indications came from PION code calculations which overestimated the neutron emission for high η_D [9]. To reproduce the observed neutron rate it was necessary to reduce, artificially, the power in the fast wave to 40% of the input power. In contrast, calculations for all discharges with $\eta_D \cong 10\%$ require no such reduction in fast wave power to reproduce the observed D-T reactivity. The experimental data support this reduction of fast wave power to the deuterons but also show that all the power is deposited in the plasma core with a large fraction flowing to thermal ions. The most likely candidate heating mechanism is mode conversion to a backward-travelling ion Bernstein wave (IBW) which is absorbed by cyclotron damping on thermal deuterons. Ion damping of an IBW has been observed in supershots in the TFTR tokamak [10], although such experiments had a higher deuterium fraction and the damping occurred on the tritons.

The highest value of $T_i(0)$ was achieved in discharge 42769 with $\eta_D \cong 18\%$ (Fig.3). For comparison, the time evolution of pulse No: 42792, at I_P = 3.7 MA, with the same RF power but with $\eta_D \cong 10\%$ and $n_e(0) \sim 4.6 \times 10^{19}$ m^{-3} is also shown. The ion pressure is greatest for the $\eta_D \cong 18\%$ case and equals the electron pressure for the $\eta_D \cong 10\%$ discharge. Furthermore, the total thermal energy contents, and their radial profiles, are almost identical in the two cases: this implies that the ICRF power deposition is the same for each discharge, and predominantly in the plasma core. Since the thermal energy contents are similar, the higher current and density in the $\eta_D \cong 10\%$ case results in a lower normalised confinement; H97 = 0.8 compared with H97 = 0.95 for the $\eta_D \cong 18\%$ case.

The Doppler broadened neutron spectra (Fig.4) clearly show a reduction in deuterium average energy resulting from the combination of higher minority concentration and reduced fast wave power absorption. The results for $\eta_D \cong 10\%$ and 18%, respectively, are the top and bottom traces; an intermediate example with $\eta_D \cong 13\%$ is also shown. The data are modelled with a deuterium distribution comprising an anisotropic Maxwellian with perpendicular and parallel temperatures $T_\perp$ and $T_{//}$, respectively, together with an isotropic thermal Maxwellian component with the measured value of $T_i(0)$. A thermal distribution is used for the tritons. The response of the spectrometer is calculated with a Monte Carlo

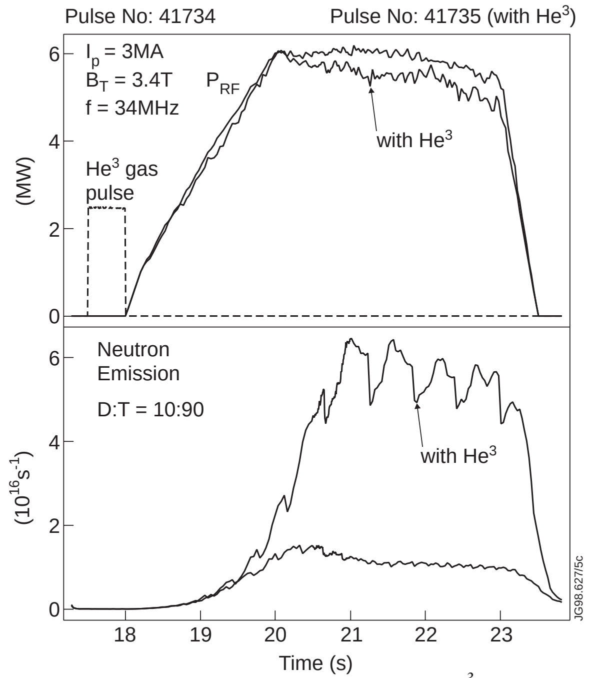

Fig. 5. Increased reactivity with 4% He^3 added to the second harmonic tritium ICRF scenario.

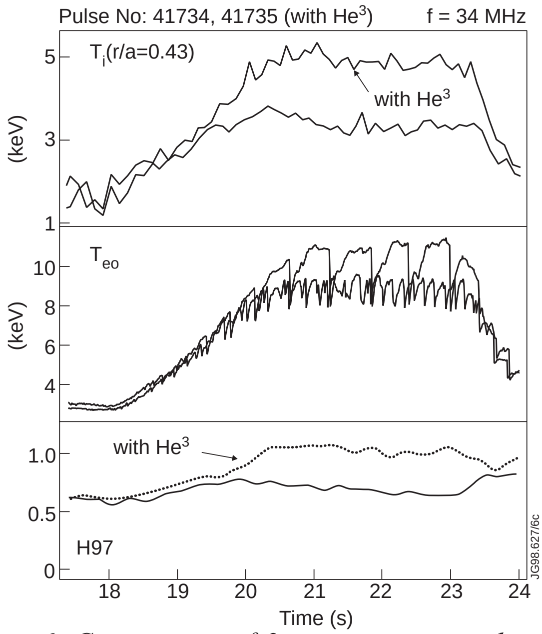

Fig. 6. Comparison of 2ω$_{CT}$ scenarios with and without He^3.

code for a range of values of $T_\perp$, $T_{//}$, and the magnitude of the thermal deuteron component, and the best values of the parameters are then determined from a χ^2 fit to the data. For $\eta_D \cong 10\%$ the suprathermal reactions dominate and the deuteron tail temperature is 100 keV in agreement with the NPA measurement (Fig.4). For $\eta_D \cong 18\%$ the thermal reactivity contributes 60% of the total. This value, derived from the least square fit, agrees well with the value of 53% calculated from the ion temperature and density profiles at 17.9s.

3. ^{3}HE MINORITY AND TRITIUM SECOND HARMONIC ICRH

Fundamental ^{3}He minority and second harmonic tritium ($2\omega_{CT}$) ICRH are competing absorption mechanisms since both resonances occur at the same position in the plasma. ^{3}He minority in D-T plasma is a strongly absorbing scheme, with increasing single pass damping as the tritium fraction increases. The $2\omega_{CT}$ absorption relies on finite Larmor radius effects to allow damping of the fast wave. The single pass absorption is typically weaker than that for ^{3}He minority in JET plasmas.

Initial experiments, carried out at 3 MA, with toroidal magnetic field of 3.4 T and central $2\omega_{CT}$ resonance in D:T=10:90 plasmas, showed strong enhancement of the neutron emission when a small amount of ^{3}He was added to the discharge (Fig.5). Discharge 41734 has no ^{3}He injection and the fast wave power is absorbed partly by tritons and partly by electrons (TTMP + ELD) according to PION calculations. About 0.1% ^{3}He will be present in the tritium from radioactive decay and could absorb up to 30% of the power in the absence of RF pump-out from the plasma centre. However, simulations of the neutron emission give best results for no power absorption by ^{3}He [9]. On the other hand, discharge 41735 has similar ICRF power but ^{3}He is injected prior to the application of the ICRH to give a concentration $n_{^3He}/n_e \approx 4\%$. In this case the neutron emission is increased fourfold to $6.5\text{x}10^{16}$ s^{-1}. Increasing the ^{3}He concentration beyond 4% produces no further improvement.

The higher reactivity observed with ^{3}He minority heating is due to the higher ion temperature (Fig.6); he density is also 30% higher in the former discharge so that the ion energy density is approximately a factor of two higher with ^{3}He minority heating. A precise comparison was not possible due to a lack of CXS $T_i(r)$ data. $T_e(0)$ is also larger in the ^{3}He minority case, mainly due to the monster sawteeth whose presence indicates a greater fast ion pressure inside the $q = 1$ surface. The H-mode factor reaches H97 = 1.1 and 0.75 with and without ^{3}He injection, respectively.

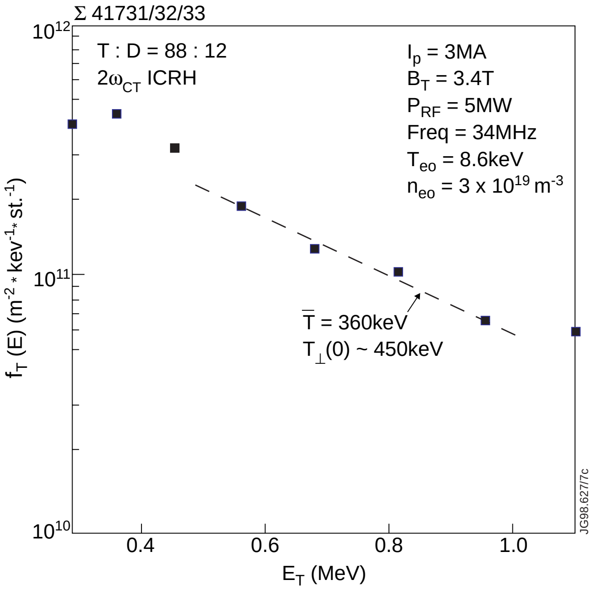

Fig. 7. Triton distribution from high energy NPA measurements. The data are the aggregate of pulses with ±90° and π antenna phasings.

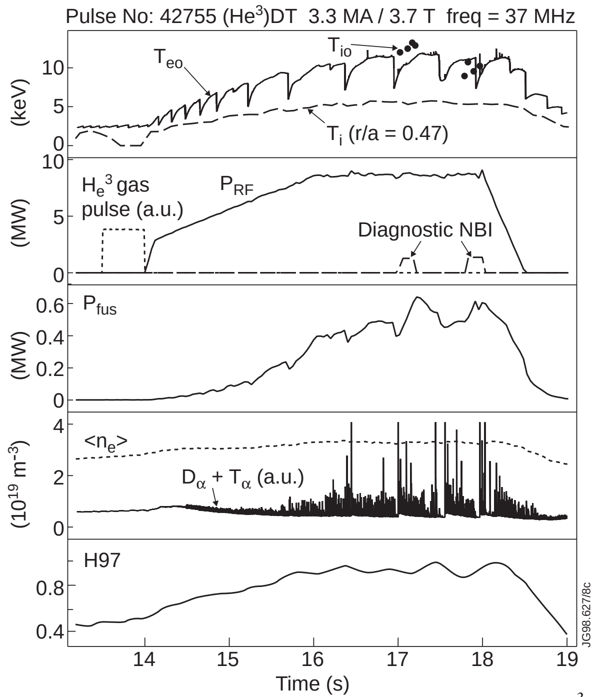

Fig. 8. Parameters for the record DT yield with He^3 minority ICRH : 10% He^3 concentration.

The reduced H-factor with 'pure' $2\omega_{CT}$ heating is understood, at least in part, to be due to the large orbits of the tritons. PION calculations show that a small number of tritons are accelerated to MeV energies. Above 4 MeV some trapped particle orbits intersect the limiters and ~ 20% of the input power is lost in this way. This loss is not included in the calculation of H97. The large triton orbits also broaden the heating profile and reduce the global confinement. The absence of monster sawteeth is consistent with a broad fast ion density profile.

With ^{3}He injection, the greater ion heating is mainly due to two factors. The strong single pass absorption by ^{3}He ions reduces the competing TTMP + ELD power flowing to the electrons, and the average energy of the ^{3}He ions is close to E_{crit} which is about 240 keV for discharge 41735. By contrast, the $2\omega_{CT}$ scheme accelerates the ions well above E_{crit} (Fig.7). Similar distributions are seen with $2\omega_{CT}$ heating in TFTR [10]. The energetic tail is due to both the longer slowing down time and the preferential absorption of power on energetic ions at second harmonic. In discharge 41734 the fast ion energy content is 1.5 MJ compared to 0.7 MJ in discharge 41735. Maximum thermal fusion reactivity was obtained from the ^{3}He minority heating scenario with a 45:55 D:T mixture in a 3.3 MA, 3.7 T discharge with 10% ^{3}He minority concentration (Fig.8). The ICRH frequency was 37 MHz and he coupled power was 8.7 MW which produced a plasma stored energy of 6 MJ corresponding to a toroidal beta of 0.9%, and a fast ion stored energy of roughly 0.7 MJ. An H-mode is triggered at 14.5 s and the ELMs increase in amplitude as the power is increased. The normalised confinement, H97, also increases with increasing power and reaches a value of 0.95 before the first diagnostic beam pulse. The value of T_i given by the X-ray spectrometer at r/a = 0.47 is similar to that in discharge 41735 (Fig.5) implying $T_{io} > T_{eo}$.

As a result of the high value of T_i the thermal neutron emission rises to $1.7x10^{17}s^{-1}$ corresponding to a fusion power of 0.5 MW. Neutron spectrometer measurements show a Doppler broadening commensurate with $T_i = 13.5 \pm 2.5$ keV in good agreement with the CXS measurement. Similar results were achieved with 6.5% ^{3}He where the T_i profiles are more peaked than the T_e profiles during the sawtooth flat top. PION calculations give similar ion and electron heating profiles, as shown in Fig 9, which suggests that the ion thermal transport in the plasma core is significantly less than the electron transport. This is confirmed by TRANSP analysis [11] which gives $\chi_i \approx 0.6\ m^2/s$ and $\chi_e \approx 2\chi_i$ at r/a = 0.2, values typical of D-T ELMy H-modes in JET. For the 10% ^{3}He case, PION shows that the ^{3}He ions take 90% of the power with 10% being deposited directly on the electrons by TTMP and ELD. Collisional power transfer from the ^{3}He gives 55% of the input power to the bulk ions and 35% to electrons.

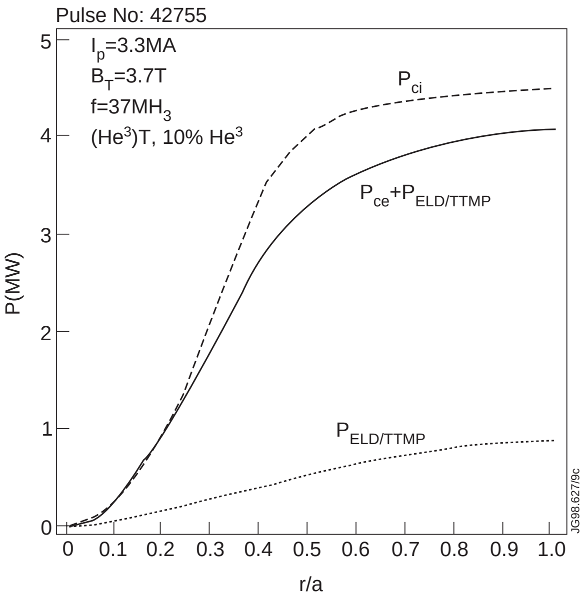

Fig. 9. PION code calculations of the power partition for 10% He^3 minority heating.

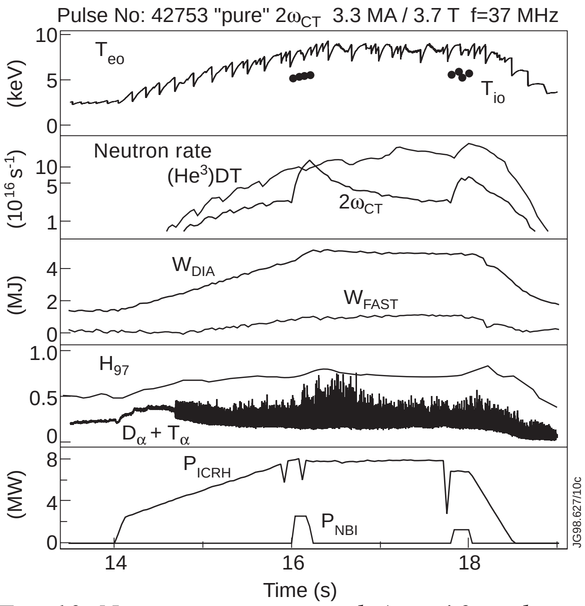

Fig. 10. Neutron reactivity with 'pure' $2\omega_{CT}$ heating and a comparable He^3 minority case. Note the logarithmic scale for the neutron rate.

The best fusion performance of the $2\omega_{CT}$ heating scheme is shown in Fig.10. This is a 3.3 MA discharge with a toroidal field of 3.7 T. The RF power was 8 MW at a frequency of 37 MHz. An H-mode is formed at 14.7s to give a normalised energy confinement, H97 = 0.7. The neutron emission rises to $2.5\times10^{16}s^{-1}$ just before the injection of the diagnostic NBI. In the core the electron temperature clearly exceeds the ion temperature. The fast ion energy content is 1 MJ which is well reproduced by PION calculations which also predict that 20% of the absorbed power is lost through tritons with energies greater than 5 MeV striking the limiters. The power distribution calculation shows that direct electron damping absorbs 55% of the power and the tritons absorb 45%. In addition the power absorbed by the tritons is collisionally redistributed mainly to the electrons. Consequently, electron heating dominates with a total of 90% of the input power going to the electrons. The energetic tritium tail excited toroidal Alfvén Eigenmodes (TAE modes) which were not observed with either the deuterium or ^{3}He minority heating. This is qualitatively consistent with the fast ion energy content being, typically, twice that in the $2\omega_{CT}$ experiments.

4. TRITIUM MINORITY HEATING

Tritium minority experiments (T)D were performed in 95:5 D:T plasmas at 3.7MA, 3.85T. The lowest ICRF frequency available in JET, 23 MHz, was used, which placed the resonance layer about 0.4m on the high field side of the magnetic axis. In this “inverted” ICRH scenario, cold plasma theory places the L cut-off between the resonance and the low field side antenna [12]. As the parallel temperature of the tritons becomes sufficient to Doppler broaden the resonance out to the cut-off, the tritons are able to absorb power from the fast wave. Calculations with the ISMENE [13] code indicate that the tritons absorb about 65% of the power, given that the average parallel energy of the deuterons is 7 keV as determined by neutron spectrometer data, the rest being absorbed directly by the electrons.

The discharge evolution is shown in Fig. 11. The power available at this frequency was severely limited by reduced coupling. The ICRF power from two antennas reaches 1.7 MW, below the H-mode threshold. $\tau_E \approx \tau$(ITER89-P), indicating that ICRF is absorbed efficiently. From the X-ray crystal spectrometer T_i(r/a=0.37) = 2 keV, close to the resonance position, consistent with the value of 2.2 keV given by the CXS measurement. The D-T neutron rate increases as the power is raised and reaches 1.5×10^{16} s^{-1}. This reaction rate is about twenty times the thermal reactivity calculated from the ion temperature and density profiles, and is due to accelerated tritons reacting with thermal deuterons. This conclusion is verified by neutron spectrometer measurements: the best fit to the data is for a triton $T_\perp = 35\pm 3.5$ keV and $T_{//} = 7.0 \pm 3.5$ keV. ICRF acceleration of tritium minority ions has also been detected in similar experiments in TFTR [14].

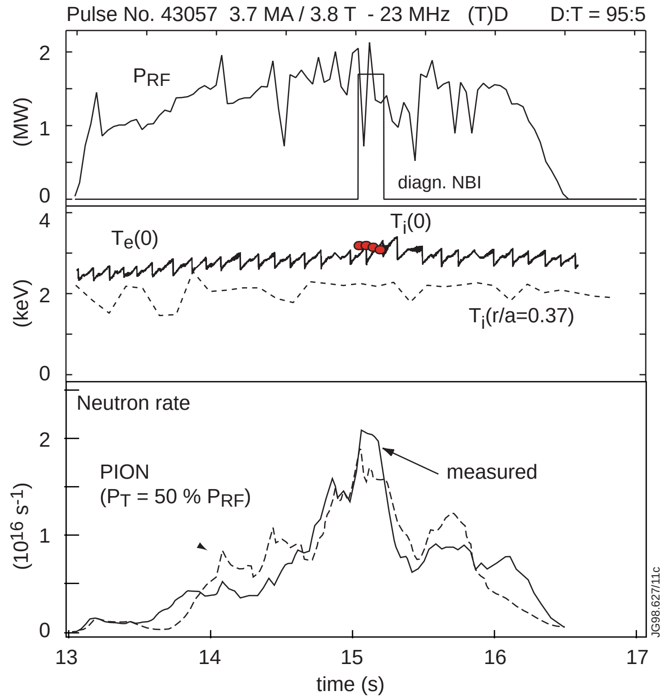

Fig. 11. Plasma parameters evolution for the (T)D scenario.

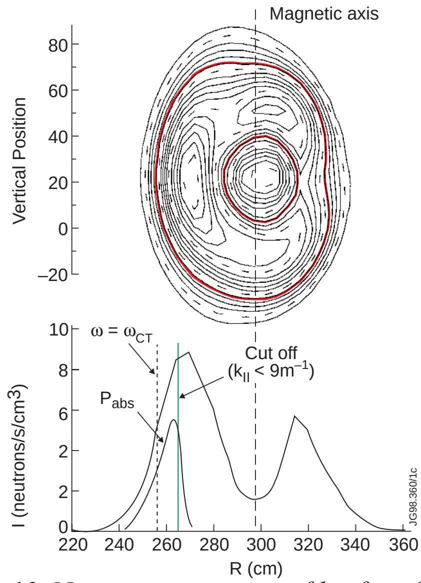

Fig. 12. Neutron emission profiles for off-axis (T)D heating. The solid curve on the contour plot corresponds approximately to the half-height.

Tomographic reconstruction of the neutron emission profile shows an annulus with the maximum emissivity occurring close to the peak power absorption as given by the ISMENE code (fig. 12). The maximum power absorption occurs near the ion-ion hybrid layer as a result of the large E_+ polarisation at this position. The asymmetry of the profile is probably due to the longer time spent by the tritons on the high field side of the magnetic axis. Orbit calculations show that 35 keV tritons close to the trapped / passing boundary spend about three times longer on the high field side of the plasma centre. The annular emission becomes more peaked as the neutron energy increases. This result implies that the highest energy tritons occupy a narrow annulus which broadens as they slow down and diffuse radially. PION calculations, with the fraction of power absorbed by the tritium as a free parameter, reproduce the neutron emission well for an absorption fraction of 50%, which is consistent with the 65% absorption by the tritons estimated by ISMENE. Most of this power is transferred collisionally to the bulk ions.

5. SUMMARY AND CONCLUSIONS

The (D)T heating scenario in a 9:91 D:T plasma produced 1.66 MW of fusion power with 6 MW of RF power, and a record steady state value of P_{FUS}/P_{IN} of 0.22. This scenario also generated substantial bulk ion heating: $T_i(0) = 10.5$ keV was achieved with $\eta_D \cong 18\%$. However, at this level of minority density the deuteron energy was so reduced as to indicate a transfer of power away from fast wave heating of the minority ions. The competing mechanism appears to be either mode conversion to an IBW, with subsequent damping by ions, or absorption by fully stripped Be^9 ions. Both mechanisms can generate the observed central bulk ion heating.

In the $2\omega_{CT}$ experiments the addition of a small amount of ^3He is sufficient to make the damping switch completely to fundamental ^3He cyclotron absorption. Strong ion heating is produced by the ^3He minority ICRH giving $T_i(0)$ up to 13 keV. This scheme is perhaps the most promising for a reactor, for which only 2-3% He^3 is required to give 70% ion heating on the route to ignition.

Both D and ^3He minority schemes have generated $T_i(0) > T_e(0)$, but the $2\omega_{CT}$ heating gives $T_e(0) > T_i(0)$. This results from both highly energetic triton tail production and strongly competitive direct electron damping for the dipole antenna phasing used in the present experiments; the average central temperature for the best $2\omega_{CT}$ discharge falls below the trend followed by the minority schemes as a consequence of the loss of energetic tritons and the orbit broadening of the heating profiles. All three heating schemes produced H-modes having small amplitude, high frequency ELMs with $\Delta W/W < 1.5\%$ which is close to the value of 1% required by a reactor. In the JET experiments, where the power density is ~1 MW/m^3, the $2\omega_{CT}$ scheme produces mainly electron heating. If, in a reactor-type plasma, the power density can be kept below 0.3 MW/m^3, e.g. by using two or more resonances to spread the power deposition, then the energy of the triton tail will be low enough to give mainly bulk ion heating. Direct electron damping can be minimised by using a value of $k_{//}$ close to 3 m^{-1}. The PION code has also been used to investigate the ^{3}He minority scheme for reactor conditions [12].

The "inverted" ICRF scheme, with 5% T minority in a D plasma, has been demonstrated as a successful heating method with about 50% of the fast wave power damped by the tritons. The tritons reached an energy of 35 keV for 1.7 MW of power and the fusion reactivity was dominated by suprathermal T-D reactions.

The JET DTE1 campaign has provided a unique opportunity to assess physics and performance of some of the ICRF scenarios envisaged for reactor plasmas. The results indicate that bulk ion heating can be provided by ICRF and that the physics picture of such scenarios is generally correct. The good level of agreement with theory and numerical modelling gives confidence in the predictions for reactor plasmas.

REFERENCES

[1] THE JET TEAM, presented by J Jacquinot, 18th EPS Conference on Plasma Physics and Controlled Fusion, Berlin, 1991.
[2] T H STIX, Nuclear Fusion, 15 (1975) 737.
[3] THE JET TEAM, presented by J Jacquinot, Plasma Physics and Controlled Fusion, 30 (1988) 1467.
[4] V P BHATNAGAR, J JACQUINOT and THE JET TEAM, Fusion Engineering and Design, 26 (1995) 575.
[5] L-G ERIKSSON et al., Proc. of the Workshop on ICRF Heating and Current Drive in D-T Plasmas, Princeton Plasma Physics Laboratory, January 1994 (Edited by J R Wilson and C K Phillips).
[6] J G CORDEY et al., Plasma Physics and Controlled Fusion, 39 (1997) B115.
[7] L-G ERIKSSON, T HELLSTEN and U WILLÉN, Nuclear Fusion 33 (1993) 1037.
[8] A A KOROTKOV, A GONDHALEKAR and A J STUART, Nuclear Fusion, 37 (1997) 35.
[9] L-G ERIKSSON, Nuclear Fusion, to be published.
[10] R MAJESKI ET al., Proc. of the 12th Topical Conf. on Radio Frequency Power in Plasmas, Savannah, 1997, p. 73.
[11] G A COTTRELL et al. and references therein, to be published in Nuclear Fusion.
[12] D.F.H. START et al. and references therein, to be published in Nuclear Fusion.
[13] K APPERT, T HELLSTEN, J VACLAVIK and L VILLARD, Comput. Phys. Commun., 40 (186) 73.
[14] C K PHILLIPS and R MAJESKI, unpublished data, private communication, 1997.